Biochemical and Biophysical Research Communications 812 (2026) 153542

Contents lists available at ScienceDirect

Biochemical and Biophysical Research Communications

journal homepage: www.elsevier.com/locate/ybbrc

The assembly of monomeric human L-lactate dehydrogenase into catalytically active homotetramer is hindered by long-chain dicarboxylates

Alessandra Stefan [a,b], Luca Gentilucci [c], Hang Liao [c], Alejandro Hochkoeppler [a,b,*]

[a] Department of Pharmacy and Biotechnology, University of Bologna, Via Gobetti 87, Bologna, 40129, Italy
[b] CSGI, University of Firenze, Via della Lastruccia 3, Sesto Fiorentino, FI, 50019, Italy
[c] Department of Chemistry "Giacomo Ciamician", University of Bologna, Via Gobetti 85, Bologna, 40129, Italy

ARTICLE INFO

Keywords:
Human lactate dehydrogenase
Dicarboxylates
Hexadecanedioic acid
Crocetin
IC_{50}

ABSTRACT

Prokaryotic and eukaryotic L-lactate dehydrogenases catalyze both the reduction of pyruvate to L-lactate and the reverse reaction generating the α-ketoacid. Remarkably, the energetic metabolism of human malignant cells is sustained by lactate dehydrogenase A (hLDH-A), the catalytic action of which is committed to its homotetrameric form (denoted hLDH-5), and is coupled to glycolysis. Therefore, hLDH-A represents a substantial druggable target, demanding the search for effective inhibitors of this enzyme.

Here we report on the inhibition of hLDH-A exerted by dicarboxylates, whose performance is strictly dependent on their carbon chain length. In particular, the best performers were tetradecanedioic acid, hexadecanedioic acid, and crocetin (a polyunsaturated dicarboxylate), whose addition to assay mixtures strongly inhibited the activity of hLDH-A. Moreover, the inhibition of hLDH-A by hexadecanedioic acid was more effective against the monomeric enzyme than towards its tetrameric counterpart, suggesting that this dicarboxylate interferes with the assembly of hLDH-5. Furthermore, docking simulations support that long-, but not short-chain dicarboxylates, effectively bind to a specific site of monomeric hLDH-A, plausibly preventing its assembly into catalytically-competent hLDH-5. Overall, our observations indicate long-chain dicarboxylates as efficient inhibitors of hLDH-A, prompting to test their action *in cellulo*.

1. Introduction

The functional ensemble of lactate dehydrogenases (LDHs) embodies quite a number of dissimilar enzymes sharing the ability to catalyze the reversible conversion of pyruvate to lactate. Notably, the diversity among the members of this functional group resides in their structural features as well as in their mode of action. It is indeed known that LDHs are characterized by dimeric or tetrameric quaternary structure, and can be assisted by β-NAD(H) or FAD(H_2) as redox cofactors [1,2]. In addition, eukaryotic cells express multiple isoforms of tetrameric LDHs, containing the LDH-A, LDH-B, or the LDH-C subunit [1]. Remarkably, it was early shown that these subunits can be assembled into homo- or hetero-tetramers, with LDH-5 and LDH-1 denoted as the homo-tetramers containing the LDH-A and the LDH-B subunit, respectively [3]. It should also be noted that LDHs exert their catalytic action according to stereospecific mechanisms, i.e. exclusively generating and oxidizing L- or D-lactate.

In human cells, LDH-1 and LDH-5 are mainly expressed in aerobic and in transiently-microaerobic tissues, respectively. Furthermore, human LDH-5 (hLDH-5) is abundantly present in malignant cells [4], whose energetic metabolism relies on aerobic glycolysis, i.e. on the generation of ATP via the glycolytic pathway coupled to the reduction of pyruvate into L-lactate. This feature of cancer cells translates hLDH-5 into an appealing druggable target, and it has accordingly prompted quite a number of strategies aiming at the suppression of hLDH-5 catalytic activity. In particular, the search for competitive inhibitors directed against hLDH-5 provided a repertoire of efficient compounds, the specificity of which was however rather poor [5]. Therefore, the lasting occurrence of this inconvenience pointed towards the identification of allosteric hLDH-5 inhibitors, leading recently to the discovery of antagonists characterized by strong specificity of action, surprisingly extended to the discrimination between LDH isoforms [6].

Importantly enough, the catalytic action of LDHs has been shown to strictly depend on their quaternary structure. Specifically, it was observed that oligomeric states containing a submaximal number of subunits are inactive or feature a lowered catalytic performance [7,8].

* Corresponding author. Department of Pharmacy and Biotechnology, University of Bologna, Via Gobetti 87, 40129, Bologna, Italy.
E-mail address: a.hochkoeppler@unibo.it (A. Hochkoeppler).

https://doi.org/10.1016/j.bbrc.2026.153542
Received 22 February 2026; Accepted 28 February 2026
Available online 5 March 2026
0006-291X/© 2026 The Authors. Published by Elsevier Inc. This is an open access article under the CC BY license (http://creativecommons.org/licenses/by/4.0/).

This implies that LDHs can be inhibited by interfering with their assembly, and suggests that this opportunity should provide specific inhibitors acting on protein-protein interactions. Accordingly, peptides were devised as appropriate tools to hinder the association of four human LDH-A (hLDH-A) subunits into hLDH-5 [9–12]. At present, the best performer among the peptides tested is cGmC9, a cyclic heptadecapeptide the IC_{50} of which was determined as equal to 2.5 μM. It should however be noted that the inhibitory action of this peptide was assayed by dissociating hLDH-5 at low pH (2.5), exposing the dissociated enzyme to cGmC9, and subsequently shifting back the pH to 7.4 [11]. To overcome this inconvenient, we isolated homogeneous monomeric hLDH-A under neutral pH conditions, and we tested quite a number of linear and cyclic peptides as candidate inhibitors of hLDH-5 assembly [12].

It was recently reported that in the absence of the allosteric effector fructose 1,6-bisphosphate (FBP) the tetrameric LDH from *Geobacillus stearothermophilus* (gsLDH) dissociates into two dimers [8]. Interestingly, this dissociation is triggered by the electrostatic repulsion that takes place, in the absence of FBP, between couples of histidines and arginines located at the dimers' interface [8]. Conversely, when FBP is present the positive charges of these amino acids engage electrostatic interactions with the phosphate groups of the effector, inducing a stabilization of the tetrameric enzyme [8]. Taking into account these observations, we considered of interest to devise an action opposite to that exerted by FBP. In particular, we reasoned that a long-stretched molecule bearing a negative charge at two distal sites represents an appealing candidate to interfere with the interactions taking place at the interface between the subunits of the oligomeric forms of hLDH-A. Accordingly, we report here on the inhibitory action exerted by dicarboxylates on the assembly and on the activity of human LDH-5, along with the outcome of docking simulations performed to identify the binding sites of the most effective antagonist.

2. Materials and methods

2.1. Materials

All reagents were purchased from Merck-Millipore (St. Louis, MO, USA).

2.2. Purification of monomeric and tetrameric hLDH-A

To isolate human LDH-A in monomeric form we obtained from Merck-Millipore purified LDH-5 (lot 0000245623, purity ≥95 %) solubilized in 20 mM Hepes, 200 mM NaCl, 10 % glycerol, pH 7.5. The tetrameric enzyme was loaded onto a Superdex 200 column (1.6 × 60 cm) previously conditioned with 10 mM Tris-HCl (pH 7.5), and gel filtration chromatography was performed at 0.6 mL/min. Under these conditions of low ionic strength, we exclusively recovered from the column monomeric LDH-A, in agreement with our previous observations [12]. Conversely, when the same Superdex 200 column was conditioned with 10 mM Tris-HCl (pH 7.5) containing 150 mM NaCl, and this NaCl-containing buffer was used to perform gel filtration, among the eluted fractions we only detected tetrameric LDH-A, i.e. LDH-5. The best fractions of both monomeric and tetrameric enzyme identified by SDS-PAGE analyses were pooled, concentrated and stored at −20 °C. Protein concentration was determined according to Bradford [13].

2.3. Activity assays

The enzyme-catalyzed reduction of pyruvate was assayed by determining the decrease in Absorbance at 340 nm related to the oxidation of β-NADH. The extinction coefficient of β-NADH at 340 nm was considered equal to $6.22 \bullet 10^3\ M^{-1}\ cm^{-1}$ [14]. All the assays were performed at 25 °C using a Cary 300 Bio spectrophotometer. Reaction mixtures contained 125 μM β-NADH and 500 μM pyruvate in 10 or 50 mM Tris-HCl (for monomeric and tetrameric enzyme, respectively, pH 7.5). When candidate inhibitors were tested, they were mixed with enzyme, and reactions were started by the addition of substrate and cofactor. To determine the K_m of LDH-A for pyruvate, the enzyme activity was assayed in the presence of 125 μM β-NADH in 10 mM Tris-HCl, pH 7.5. Stock solutions of pimelic, suberic, azelaic, and sebacic acid were prepared in ethanol. Therefore, when these compounds were tested as potential inhibitors of LDH-A appropriate control reactions were performed in the presence of ethanol (≤0.2 %, v/v). Tetradecanedioic, hexadecanedioc acid and crocetin were dissolved in dimethylsulfoxide (DMSO). The inhibitory action of these compounds was assayed and compared with the effect on enzyme activity triggered by DMSO only (≤0.2 %, v/v).

2.4. Structural analysis and inspection of ligand-protein interactions

The quaternary structure of human lactate dehydrogenase bound to β-NADH and oxamate (PDB file 1i10) was inspected and represented using the PyMol software [15]. To perform docking simulations, β-NADH, oxamate, and water molecules were removed from chain B of this quaternary structure. The 3D structure of azelaic acid and hexadecanedioic acid were sourced from the PubChem database (https://pubchem.ncbi.nlm.nih.gov). The structures were initially downloaded in SDF 3D conformer format and converted to mol2 format using Discovery Studio 2025. Docking studies were performed using SwissDock (https://www.swissdock.ch, [16]), a computational tool which implements the EADock DSS docking engine that allows exploring the conformational space of the ligand, and determining the best orientations in the active site of the target protein. In addition, SwissDock provides a built-in option that takes the flexibility of amino acid side chains into account. Two distinct molecular docking tools, AutoDock Vina and Attracting Cavities, were employed, due to their complementary methodological strengths. AutoDock Vina applies empirical scoring functions and a Lamarckian genetic algorithm to efficiently identify the most energetically stable and reliable binding conformations. Attracting Cavities method utilizes a surface-based energy grid approach that emphasizes molecular surface complementarity, and it was utilized for revealing interaction regions or binding poses that might not be detected using AutoDock Vina alone. The entire surface of chain B of hLDH-5 was explored by applying a search box of 20 × 20 × 20 $Å^3$ and 10 random initial conditions were selected. The best binding mode of each molecule was selected according to the lowest binding free energy (ΔG AutoDock Vina, in kcal/mol). Ligand-protein Interactions and docking results were inspected and analyzed with BIOVIA Discovery Studio v25.1.0.24284 and PacDOCK [17]. In particular, PacDOCK allows automatic atom matching and RMSD calculation (ProRMSD module), cluster analysis of docked poses (ClusDOCK module), and docking results visualization (PacVIEW module).

3. Results and discussion

As previously mentioned, it was recently shown that the allosteric effector FBP enhances the stability of tetrameric gsLDH by neutralizing the electrostatic repulsion that arginines and histidines introduce between gsLDH subunits [8]. Moreover, the increased stability of tetrameric gsLDH translates into a k_{cat}/K_m value which is threefold higher respect the corresponding parameter featured by the dimeric form of the enzyme [8]. To check if the interface between the subunits of hLDH-5 contains amino acids potentially responsible for their mutual electrostatic repulsion, we inspected the enzyme quaternary structure. In particular, we analyzed the structure of the ternary complex LDH-5/β-NADH/oxamate reported by Read et al. ([18], PDB file 1i10). Interestingly, two couples of acetate ions were detected between two interlocked dimers of hLDH-A, with each couple engaging electrostatic interactions with neighbouring histidines and arginines (e.g. between

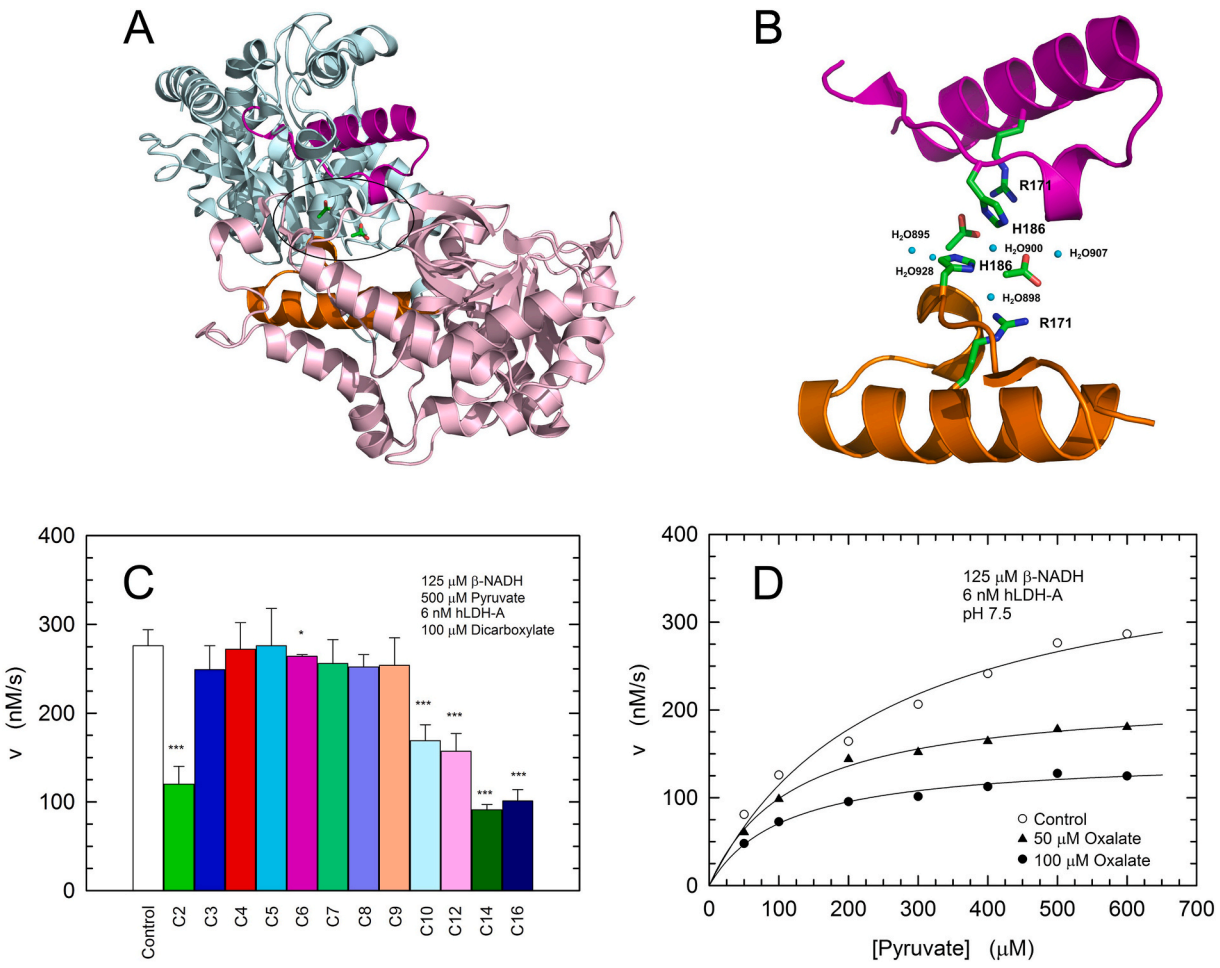

Fig. 1. Structural and functional properties of human LDH-A.
(A) The interface between two subunits of tetrameric hLDH-A is shown (PDB file 1i10). The subunits corresponding to the C and A chains are represented in cyan and salmon, respectively. The structural elements containing the histidines and arginines interacting with a couple of acetate ions are reported in magenta and orange. An ellipsoid delimits the area where the two acetates are located. (B) Detail of the structural region containing the amino acids interacting with the pair of acetate ions. The coordinates of the amino acids are numbered by considering at site 1 the formyl-methionine of the primary structure. (C) Inhibitory action exerted, if any, on monomeric hLDH-A by dicarboxylic acids. Activity assays were performed in the absence (white bar) or in the presence of 100 μM dicarboxylic acid: oxalic, malonic, succinic, glutaric, adipic, pimelic, suberic, azelaic, sebacic, dodecanedioic, tetradecanedioic, and hexadecanedioic (green, blue, red, cyan, magenta, light green, light blue, light red, light cyan, light magenta, dark green, and dark blue, respectively). Three independent assays were performed for each sample in the presence of 125 μM β-NADH, 500 μM pyruvate and 6 nM monomeric hLDH-A. Error bars represent standard deviation (n = 3). The experimental observations were compared by Student's test. The ***, and * symbols denote *p* values lower than 0.001, and 0.1, respectively. (D) Dependence of the initial velocity of β-NADH oxidation observed as a function of pyruvate concentration, in the presence of 125 μM β-NADH, 6 nM monomeric hLDH-A, and in the absence (empty circles), or in the presence of 50 or 100 μM oxalate (filled triangles and circles, respectively). The continuous lines represent the best fit of the Michaelis-Menten equation to the experimental observations. (For interpretation of the references to colour in this figure legend, the reader is referred to the Web version of this article.)

chains A and C, Fig.s 1A and 1B). Furthermore, the location of histidines and arginines in this structural region of hLDH-5 resembles the arrangement of the corresponding amino acids of gsLDH (Supplementary Fig. S1). This resemblance does indeed translate into similar distances between the α-carbon of histidines or arginines and the phosphorus atoms of FBP or the C_2 carbon of acetate (Supplementary Table ST1).

The maintenance of an appropriate quaternary structure is of high importance for the catalytic action exerted by lactate dehydrogenases [7,8]. Accordingly, we reasoned that elongated molecules bearing a negative charge at both their termini might spread apart the histidines/arginines couples at the dimer-dimer interface of hLDH-5, therefore inhibiting its activity. In particular, to test this idea we selected, as candidate inhibitors, dicarboxylates featuring carbon chains of different length. It should also be noted that the addition of β-NADH and pyruvate to monomeric hLDH-A induces its assembly into hLDH-5, as we have previously shown by means of gel filtration experiments [12]. Therefore, the extent of LDH activity detected with the assays reported here represents the output of the competition between substrates and dicarboxylates in favouring and inhibiting the assembly of hLDH-5, respectively. It was previously reported that 20 μM oxalate inhibits by 30 % the reduction of pyruvate to lactate exerted by hLDH-5 [19]. Accordingly, and not surprisingly, the addition of 100 μM oxalate to reaction mixtures was found to strongly inhibit the catalytic action of hLDH-A, whose extent was observed to decrease by 60 % (Fig. 1C). However, and to our surprise, we did not detect any significant effect triggered on LDH-A activity by 100 μM malonate, a dicarboxylate containing only a single carbon atom in addition to those making up oxalate (Fig. 1C). Similarly to what we observed with malonate, dicarboxylic acids containing 4-9 carbon atoms (succinic, glutaric, adipic, pimelic, suberic, and azelaic, respectively) were found devoid of any substantial inhibitory action on the activity of hLDH-A (Fig. 1C). Nevertheless, dicarboxylic acids featuring 10 or 12 carbon atoms (sebacic and dodecanedioic acid, respectively) were found to inhibit about 40 % of

Table 1
Kinetic parameters of monomeric and tetrameric human LDH-A.

Inhibitor	Monomeric human LDH-A			Tetrameric human LDH-A (LDH-5)		
	K_m (μM)	V_{max} (nM/s)	k_{cat} (s^{-1})	K_m (μM)	V_{max} (nM/s)	k_{cat} (s^{-1})
None	248 ± 48	399 ± 32	67 ± 5	231 ± 33	798 ± 49	133 ± 8
50 μM oxalate	120 ± 11	218 ± 6	36 ± 1	99 ± 11	343 ± 10	57 ± 2
100 μM oxalate	108 ± 15	147 ± 6	25 ± 1	71 ± 12	256 ± 10	43 ± 2
None	241 ± 24	454 ± 18	76 ± 3	289 ± 48	693 ± 51	116 ± 9
3 μM C16	172 ± 39	244 ± 20	41 ± 3	-	-	-
5 μM C16	-	-	-	931 ± 329	871 ± 220	145 ± 37
25 μM C16	143 ± 46	140 ± 15	23 ± 2	-	-	-
100 μM C16	-	-	-	1080 ± 289	976 ± 185	163 ± 31
200 μM C16	158 ± 81	51 ± 9	9 ± 2	-	-	-

The enzymatic catalytic action was assayed as a function of pyruvate concentration in the presence of 125 μM β-NADH and 6 nM enzyme.

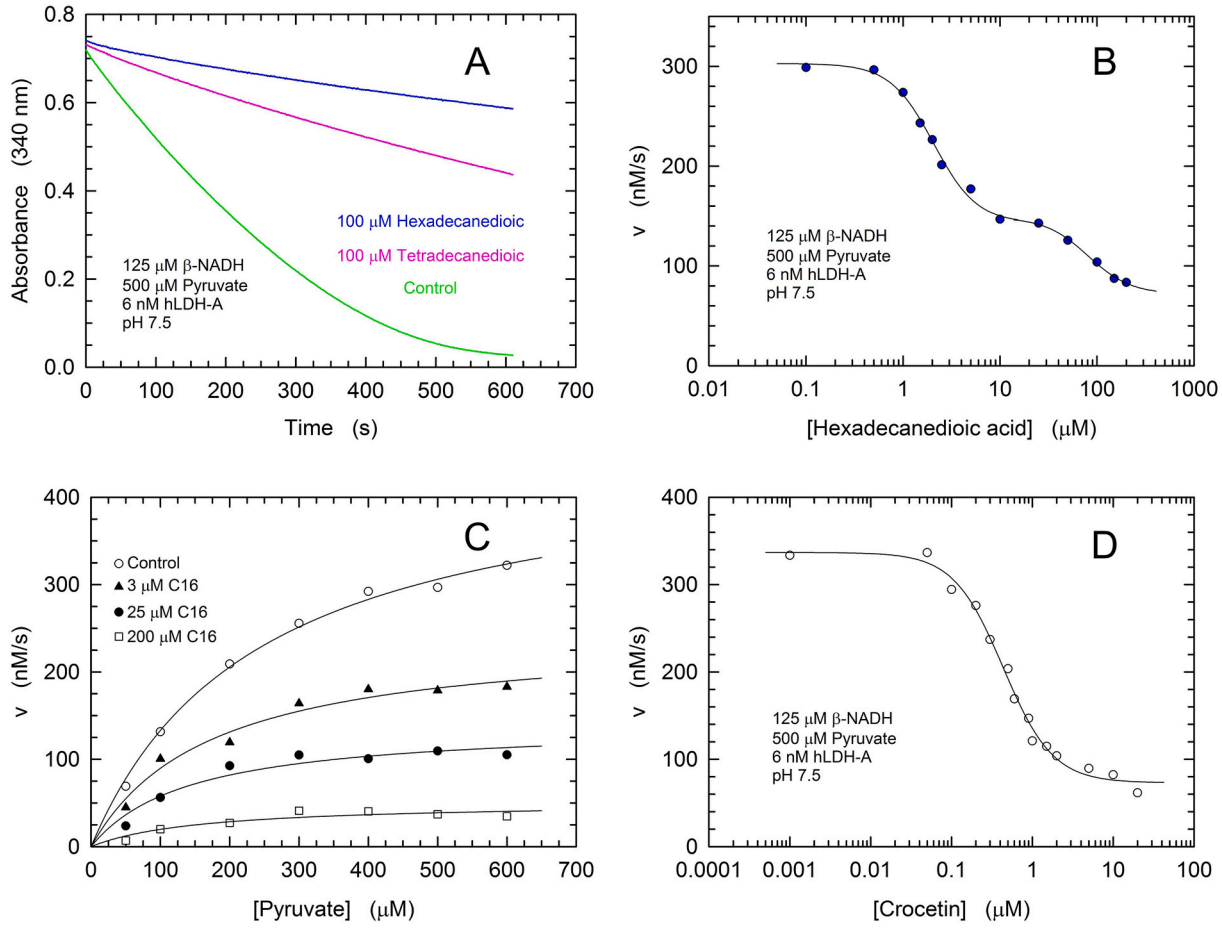

Fig. 2. Inhibition of monomeric hLDH-A by dicarboxylic acids.
(A) Kinetics of β-NADH oxidation detected in the absence (green line) or in the presence of 100 μM tetradecanedioic or hexadecanedioic acid (magenta and blue line, respectively). Assay mixtures contained 125 μM β-NADH, 500 μM pyruvate, 6 nM monomeric hLDH-A, and 10 mM Tris-HCl (pH 7.5). (B) Inhibition of monomeric hLDH-A activity as a function of hexadecanedioic acid concentration. (C) Dependence of the initial velocity of β-NADH oxidation observed as a function of pyruvate concentration, in the presence of 125 μM β-NADH, 6 nM monomeric hLDH-A, and in the absence (empty circles), or in the presence of 3, 25, or 200 μM hexadecanedioic acid (filled triangles, filled circles, and empty squares, respectively). The continuous lines represent the best fit of the Michaelis-Menten equation to the experimental observations. (D) Inhibitory action exerted by crocetin on the catalytic activity of monomeric hLDH-A. The continuous line represents the best fit of the four-parameter logistic equation to the experimental observations. (For interpretation of the references to colour in this figure legend, the reader is referred to the Web version of this article.)

the hLDH-A activity detected in their absence (Fig. 1C). In addition, tetradecanedioic (C14) and hexadecanedioc (C16) acid were responsible for the decrease of hLDH-A activity by 70 % compared to the level determined for the control sample (Fig. 1C).

To investigate the mechanism of action exerted by oxalate on monomeric hLDH-A, we estimated the kinetic parameters of the enzyme, in the absence and in the presence of this dicarboxylate. By performing activity assays as a function of pyruvate concentration, we obtained values for K_m and k_{cat} respectively equal to 248 ± 48 μM and 67 ± 5 s^{-1} (Fig. 1D–Table 1). These values translated into 120 ± 11 μM and 36 ± 1 s^{-1} when 50 μM oxalate was added to reaction mixtures (Fig. 1D–Table 1). Furthermore, in the presence of 100 μM oxalate K_m and k_{cat} were determined as equal to 108 ± 15 μM and 25 ± 1 s^{-1}, respectively (Fig. 1D–Table 1). Accordingly, oxalate acts on hLDH-A as

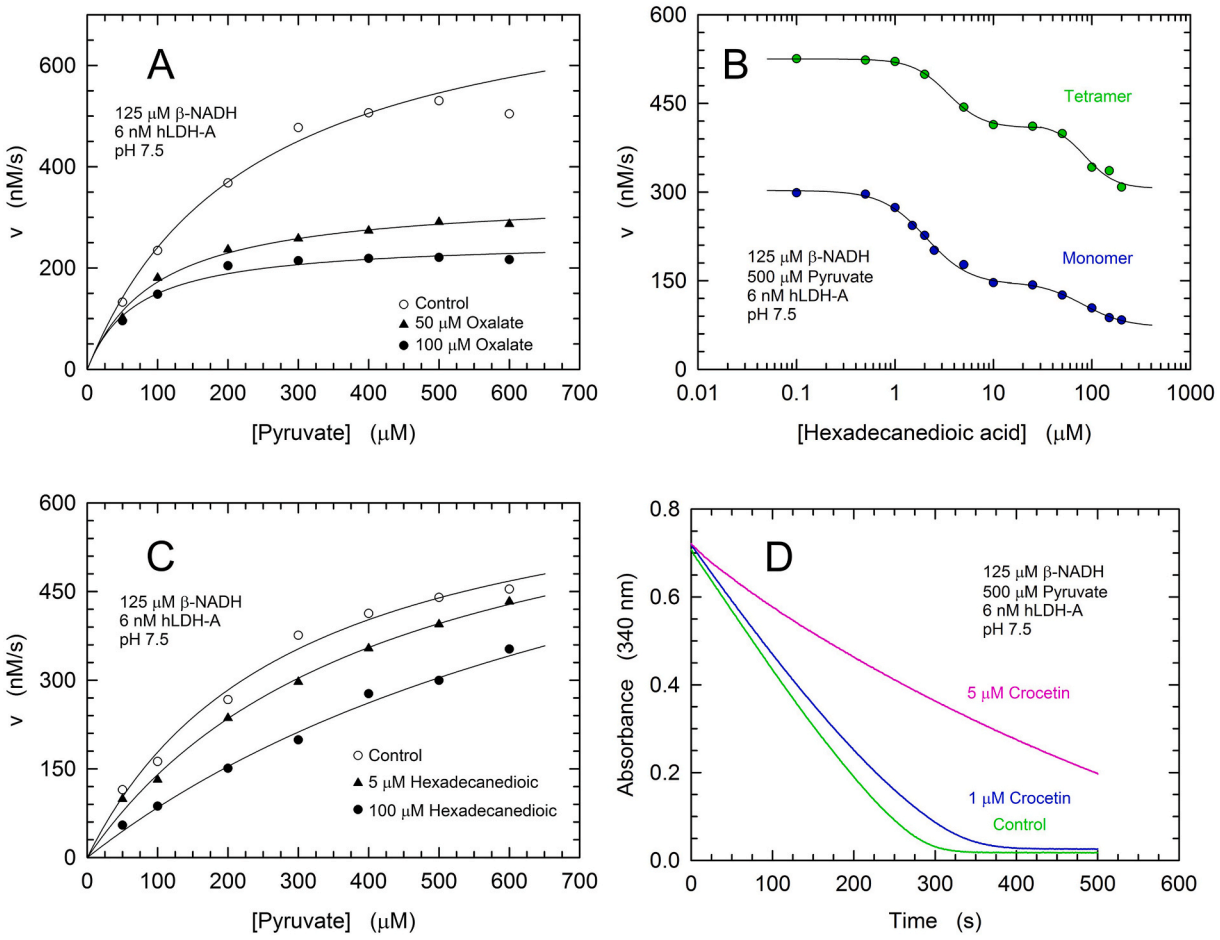

Fig. 3. Inhibition of tetrameric hLDH-A by oxalate, hexadecanedioc acid, and crocetin.
(A) Dependence of the initial velocity of β-NADH oxidation observed as a function of pyruvate concentration, in the presence of 125 μM β-NADH, 6 nM tetrameric hLDH-A (hLDH-5), and in the absence (empty circles), or in the presence of 50 or 100 μM oxalate (filled triangles and circles, respectively). The continuous lines represent the best fit of the Michaelis-Menten equation to the experimental observations. (B) Inhibition of hLDH-5 (green circles) and monomeric hLDH-A (blue circles) activity as a function of hexadecanedioic acid concentration. (C) Dependence of the initial velocity of β-NADH oxidation observed as a function of pyruvate concentration, in the presence of 125 μM β-NADH, 6 nM hLDH-5, and in the absence (empty circles), or in the presence of 5 or 100 μM hexadecanedioic acid (filled triangles and circles, respectively). The continuous lines represent the best fit of the Michaelis-Menten equation to the experimental observations. (D) Inhibitory action exerted by 1 or 5 μM crocetin (blue and magenta lines, respectively) on the catalytic activity of hLDH-5. (For interpretation of the references to colour in this figure legend, the reader is referred to the Web version of this article.)

an uncompetitive inhibitor, presumably binding to the enzyme-NADH-pyruvate ternary complex. This mode of action suggests that oxalate does not impair the assembly of monomeric hLDH-A into hLDH-5, the building up of which is promoted by the binding of β-NADH and pyruvate [12].

When the initial velocity of the reaction catalyzed by hLDH-A was assayed, the inhibitory effect triggered by 100 μM C14 or C16 dicarboxylate was essentially identical (Fig. 1C). To further investigate how these two compounds affect the reaction kinetics, we observed the oxidation of β-NADH over a time interval long enough to reach the equilibrium under control conditions. Surprisingly, after an initial short phase (10-20 s) featuring a similar rate in the presence of tetradecanedioc or hexadecanedioic acid, the oxidation of β-NADH was found to be more severely inhibited by the C16 dicarboxylate (Fig. 2A). In particular, when a double-exponential equation was fit to the experimental observations, the major difference between the effects promoted by the two dicarboxylates resides in the amplitude of the reaction, which is contained to the oxidation of 61 μM of β-NADH in the presence of hexadecanedioic acid (Supplementary Fig. S2, Table ST2). Interestingly, when the inhibition of monomeric hLDH-A was determined as a function of the concentration of this dicarboxylic acid we detected a biphasic dependence (Fig. 2B). We interpret this peculiar feature as due to: i) the interference by the C16 dicarboxylate on the assembly of hLDH-5, with this effect being predominant at low inhibitor concentrations; ii) the inhibition of hLDH-5 catalytic action, mainly taking place at high hexadecanedioic acid concentrations. To further ascertain this point, we determined the kinetic parameters of monomeric hLDH-A in the absence and in the presence of hexadecanedioic acid. Overall, the C16 dicarboxylate was found to be responsible for a strong decrease of k_{cat}, the value of which was lowered down by almost one order of magnitude at 200 μM hexadecanedioic acid (Fig. 2C–Table 1). Contrary to this, the enzyme K_m for pyruvate was slightly affected, if at all, by the C16 dicarboxylate (Fig. 2C–Table 1), indicating that hexadecanedioic acid represents a non-competitive inhibitor of monomeric hLDH-A.

Crocetin is a dicarboxylic acid the unsaturated carbon chain of which contains 16 carbon atoms, along with four branching points and seven conjugated double bonds. Considering the effectiveness of hexadecanedioic acid against hLDH-A activity, we selected crocetin as a further candidate inhibitor. Remarkably, crocetin was found to be extremely effective in inhibiting monomeric hLDH-A, featuring a value of IC_{50} equal to 436 ± 36 nM (Fig. 2D). It should be noted that this value is significantly lower than that reported for the inhibition of hLDH-5, i.e. 54.9 ± 4.7 μM [20]. Furthermore, it should be mentioned that we tested crocin, which is the digentiobiose ester of crocetin. Interestingly, crocin

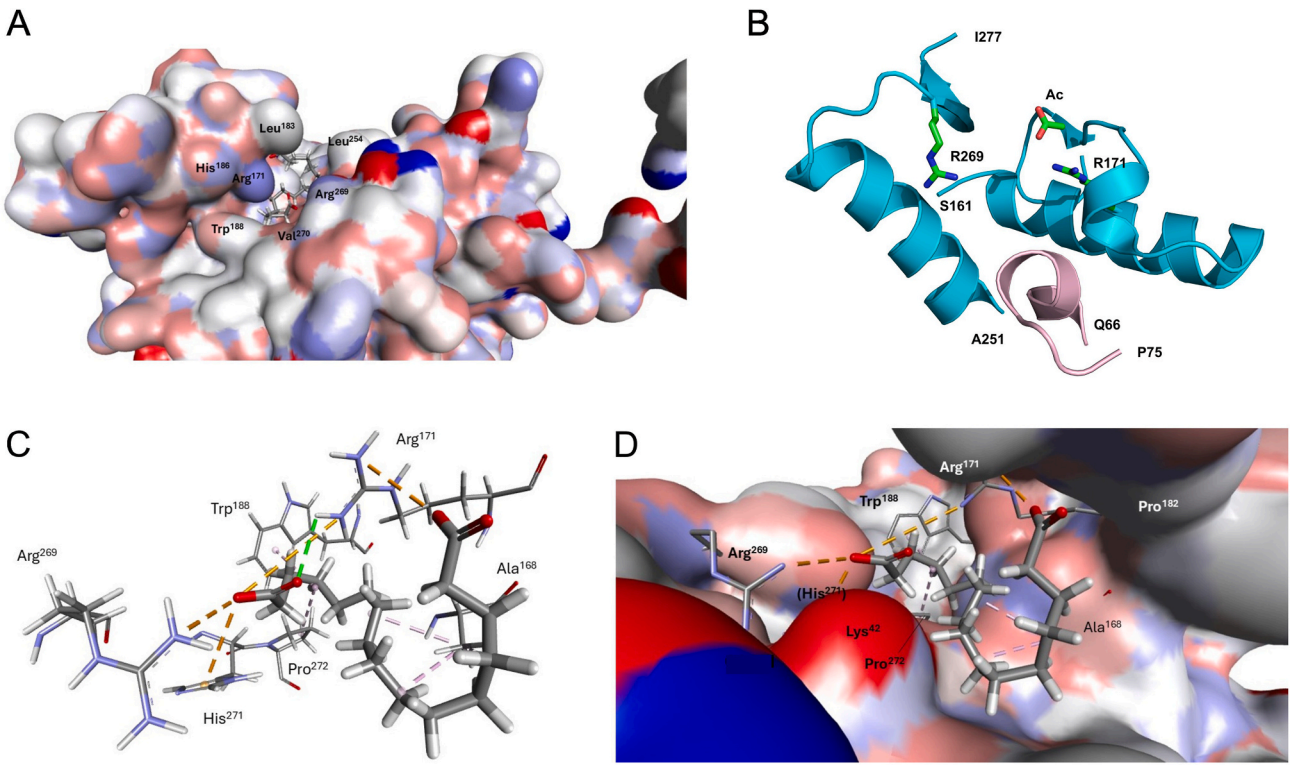

Fig. 4. Interactions of hexadecanedioic acid with hLDH-A.
(A) Binding mode of hexadecanedioic acid to chain B of hLDH-5 corresponding to the best stability of the enzyme-ligand complex. The dicarboxylate lying down on the protein surface is represented with sticks. (B) The region of chain A of hLDH-5 spanning residues 66-75 and located into a crevice of chain B (represented in cyan) is shown in salmon. (C,D) Main interactions engaged by hexadecanedioic acid (reported with sticks) with chain B of hLDH-5. Intra- and inter-molecular interactions are designated with light grey and yellow dashed sticks, respectively. A hydrogen bond between R171 and hexadecanedioic acid is shown with a green dashed stick. (For interpretation of the references to colour in this figure legend, the reader is referred to the Web version of this article.)

was found ineffective against hLDH-A (Supplementary Fig. S3), suggesting that the action of crocetin is strictly dependent on its free dicarboxylic groups.

The previous observation that crocetin is competent in inhibiting hLDH-5 [20] prompted us to test the action of dicarboxylates against tetrameric hLDH-A. Remarkably, oxalate was determined to be an uncompetitive inhibitor of hLDH-5 (Fig. 3A) and, quantitatively speaking, its effect on the tetrameric enzyme was comparable to that detected on monomeric hLDH-A (cf. Fig.s 1D–3A, Table 1). Conversely, hexadecanedioic acid was observed to be less effective on hLDH5 than against its monomeric counterpart (Fig. 3B). Moreover, the C16 dicarboxylate did only alter the K_m of hLDH-5 for pyruvate, the enzyme k_{cat} being unaffected even in the presence of 100 μM of hexadecanedioic acid (Fig. 3C–Table 1). Therefore, hexadecanedioic acid acts on hLDH-5 as a competitive inhibitor, with this feature in sharp contrast with the non-competitive inhibition exerted on monomeric hLDH-A. In addition to this, we observed that crocetin is less effective in antagonizing the activity of hLDH-5 than in targeting monomeric hLDH-A (Fig. 3D, cf. with Supplementary Fig. S4).

To explain the different effects exerted by long- vs. short-chain dioic acids, we performed molecular docking analyses using the tertiary structure of hLDH-5 chain B (PDB file: 1i10), and the 3D structures of azelaic acid and hexadecanedioic acid as sourced from the PubChem database. The best-score pose calculated for hexadecanedioic acid (−4.705 kcal/mol) shows the diacid located within the cavity delimited by the α-helices 164-178 and 250-264, and by the residues 265-275 and 179-191 (Figs 4A–4B). In the tetrameric complex, this cavity is fully occupied by the helix-loop 68-74 of the adjacent chain A (Fig. 4B). The enzyme-dicarboxylate complex is stabilized by several strong interactions (Figs 4C–4D). One carboxylate group interacts with Arg171 by a salt bridge, while the other carboxylate is located between Arg171 and Arg269, forming salt bridges with both guanidinium groups. The second carboxylate also interacts with His271 by a pi-anion interaction. As for the dicarboxylate carbon chain, it is located within a hydrophobic pocked delimited by the residues Pro272, Val270, Leu254, Trp188, Ala168. In contrast to what determined for hexadecanedioic acid, simulations performed for azelaic acid reveal that this molecule is capable to access into deep cavities, plausibly due to the shorter carbon chain. The best-score pose (−4.726 kcal/mol) shows the diacid placed on the rear side of the protein respect to the binding site of hexadecanedioic acid, completely buried within the protein surface (Supplementary Fig. S5), held in place by strong interactions, in particular by the salt bridges with Arg99, Arg106, and Arg169. These findings suggest that azelaic acid does not alter the profile of the protein surface, and hence it cannot prevent the intersubunit interactions responsible for the assembly of monomeric hLDH-A into tetrameric hLDH-5.

4. Concluding remarks

We reported here that long-chain dicarboxylates inhibit the assembly of monomeric hLDH-A into its catalytically-active tetrameric counterpart. In addition, in silico analyses were performed to elucidate these findings. Interestingly, when dicarboxylic acids were orally-administered to human subjects, their retention was positively affected by the carbon chain length [21]. Accordingly, long-chain dicarboxylates represent appealing candidates for targeting hLDH-A and, in turn, the energetic metabolism of cancer cells.

Funding sources

This research did not receive any specific grant from funding agencies in the public, commercial, or not-for-profit sectors.

CRediT authorship contribution statement

Alessandra Stefan: Investigation. **Luca Gentilucci:** Conceptualization, Investigation. **Hang Liao:** Investigation. **Alejandro Hochkoeppler:** Conceptualization, Investigation.

Declaration of competing interest

The authors declare that they have no known competing financial interests or personal relationships that could have appeared to influence the work reported in this paper.

Appendix A. Supplementary data

Supplementary data to this article can be found online at https://doi.org/10.1016/j.bbrc.2026.153542.

References

[1] M.E. Cristescu, et al., D- and L-lactate dehydrogenases during invertebrate evolution, BMC Evol. Biol. 8 (2008) 268.
[2] E.I. Garvie, Bacterial lactate dehydrogenases, Microbiol. Rev. 44 (1980) 106–139.
[3] C.L. Markert, Lactate dehydrogenase isozymes: dissociation and recombination of subunits, Science 140 (1963) 1329–1330.
[4] Q. Zhang, et al., A systematic pan-cancer analysis identifies LDHA as a novel predictor for immunological, prognostic, and immunotherapy resistance, Aging 16 (2024) 8000–8018.
[5] D. Sharma, M. Singh, R. Rani, Role of LDH in tumor glycolysis: regulation of LDHA by small molecules for cancer therapeutics, Semin. Cancer Biol. 87 (2022) 184–195.
[6] A. Friberg, et al., Structural evidence for isoform-selective allosteric inhibition of lactate dehydrogenase A, ACS Omega 22 (2020) 13034–13041.
[7] R. Hermann, R. Jaenicke, R. Rudolph, Analysis of the reconstitution of oligomeric enzymes by crosslinking with glutaraldehyde: kinetics of reassociation of lactic dehydrogenase, Biochemistry 20 (1981) 5195–5201.
[8] H. Cai, et al., Allosteric regulation of L-lactate dehydrogenase: beyond effector-mediated tetramerization, Protein Sci. 34 (2025) e70206.
[9] F. Jafary, et al., Novel peptide inhibitors for lactate dehydrogenase A (LDHA): a survey to inhibit LDHA activity via disruption of protein-protein interaction, Sci. Rep. 9 (2019) 4686.
[10] L. Thabault, et al., Interrogating the lactate dehydrogenase tetramerization site using (stapled) peptides, J. Med. Chem. 63 (2020) 4628–4643.
[11] F. Nadal-Bufi, et al., Designed β-hairpins inhibit LDH5 oligomerization and enzymatic activity, J. Med. Chem. 64 (2021) 3767–3779.
[12] A. Stefan, et al., Peptides inhibiting the assembly of monomeric human L-lactate dehydrogenase into catalytically active homotetramer decrease the synthesis of lactate in cultured cells, Protein Sci. 33 (2024) e5161.
[13] M.M. Bradford, A rapid and sensitive method for the quantitation of microgram quantities of protein utilizing the principle of protein-dye binding, Anal. Biochem. 72 (1976) 248–254.
[14] C. Bernofsky, S.C. Wanda, Formation of reduced nicotinamide adenine dinucleotide peroxide, J. Biol. Chem. 257 (1982) 6809–6817.
[15] W.L. DeLano, Use of PyMol as a communications tool for molecular science, Abstr. Pap. Am. Chem. Soc. 228 (2004) U313–U314.
[16] M. Bugnon, et al., SwissDock 2024: major enhancements for small-molecule docking with attracting cavities and AutoDock Vina, Nucleic Acids Res. 52 (2024) W324–W332.
[17] J. Carbone, et al., PacDOCK: a web server for positional distance-based and interaction-based analysis of docking results, Molecules 27 (2022) 6884.
[18] J.A. Read, et al., Structural basis for altered activity of M- and H-isozyme forms of human lactate dehydrogenase, Proteins 43 (2001) 175–185.
[19] P.M. Emerson, J.H. Wilkinson, W.A. Withycombe, Effect of oxalate on the activity of lactate dehydrogenase isoenzymes, Nature 202 (1964) 1337–1338.
[20] C. Granchi, et al., Characterization of the saffron derivative crocetin as an inhibitor of human lactate dehydrogenase 5 in the antiglycolytic approach against cancer, J. Agric. Food Chem. 65 (2017) 5639–5649.
[21] S. Passi, et al., Metabolism of straight saturated medium chain length (C9 to C12) dicarboxylic acids, J. Lipid Res. 24 (1983) 1140–1147.